LIMNOLOGY
and
OCEANOGRAPHY: METHODS

Limnol. Oceanogr.: Methods 7, 2009, 287–303

Evaluation of oscillating grids and orbital shakers as means to generate isotropic and homogeneous small-scale turbulence in laboratory enclosures commonly used in plankton studies

Òscar Guadayol,[1] Francesc Peters,[1] Jan Erik Stiansen,[2] Cèlia Marrasé,[1] Atle Lohrmann[3]*
[1]Institut de Ciències del Mar (CSIC), Barcelona, Catalunya, Spain
[2]Institute of Marine Research, Bergen, Norway
[3]Nortek A/S, Oslo, Norway

Abstract

The effects of turbulent motion on planktonic organisms have mainly been studied in the laboratory with devices capable of generating controlled turbulent conditions. Owing to technical and logistical difficulties, thorough assessments of hydrodynamics in such experiments are not routinely made. In this study, we examined the suitability of two widely used systems to generate isotropic, homogeneous, and stationary turbulence in laboratory containers: oscillating grid devices with large stroke length and relatively low frequencies of oscillation and orbital shaker tables. Turbulent kinetic energy dissipation rates were estimated from velocity measurements made with acoustic Doppler velocimeters. Both systems were shown to generate isotropic conditions in a relatively broad range of dissipation rates. Grid-stirred tanks produce homogeneous turbulence in both the horizontal and vertical dimensions, as long as stroke length is comparable to the height of the container. Turbulence in orbital shakers is not completely homogeneous, as it depends on the distance to the wall and to the surface. Empirical models are derived as a tool for the calculation of dissipation rates in the two systems within the ranges and conditions examined in this study.

Introduction

Turbulent flow is ubiquitous in aquatic systems and thus can potentially affect a wide range of planktonic organisms and processes. Turbulence is still often referred to as one of the unsolved problems in physics, and there has been a strong interest in its effects on plankton, especially during the last 20 years, resulting in a growingly active area of study (for a review, see Peters and Marrasé 2000). Field studies on the effects of turbulence on plankton have been hindered by the lack of turbulence measurements in biological studies and by the difficulty of discriminating these effects from those of other variables, such as temperature, light, or nutrient concentration, which often covary. Therefore, much of the current knowledge has been derived from laboratory or enclosed systems, with configurations to generate controlled turbulence conditions.

Ideally, the generation of small-scale turbulence in laboratory containers should conform to a few requirements to correctly assess the response of plankton to a certain level of turbulence in open water (i.e., not considering responses to turbulence close to bottom boundary layers). First, turbulence should be constant, that is, stationary in time and homogeneous in space. Although plankton experiences shifting turbulent conditions in nature, it is necessary to establish the responses to constant levels of turbulence before much more challenging nonstationary fields can be addressed. Second, the system should not induce changes in the behavior or distribution of the organisms other than those directly triggered by water motion. And finally, organisms must perceive turbulence as "natural." This implies, for example, that all relevant scales influencing the investigated process should be contained in the fully developed cascade of turbulent eddies (i.e., within the inertial subrange of the turbulent energy spectrum). This is difficult since the scales of generation of turbulent

*Corresponding author: E-mail: oscar@guadayol.cat
College of Oceanic and Atmospheric Sciences, Oregon State University, Corvallis, OR, USA

Acknowledgments

Thore Thoresen at Nortek A/S built the transducer array into the container where the grid turbulence was generated. David Cruz helped with the measurements in the oscillating grid containers. O.G. received a Spanish CSIC-I3P fellowship sponsored by INNOVA Oceanografía Litoral, S.L. We thank Oswaldo López for his support. We also thank Rafel Simó and Silvia de Diago for lending us two of the orbital shakers used in this study. This study was supported by the EU project NTAP (EVK3-CT-2000-00022) and by the Spanish projects TURFI (REN2002-01591/MAR) and VARITEC (REN2003-08071-C02-01/MAR). This is an ELOISE (European Land Ocean Interaction Studies) contribution.

motion in the field are much larger than in the containers used for experiments (Sanford 1997). One needs to be aware of the dimensions of the organisms and the process under study with respect to the dimensions of the container. Thus, a container used to study fish larvae/zooplankton contact rates must be much larger (relevant scales tens of centimeters to meters) than a container used to study nutrient uptake by phytoplankton (relevant scales millimeters to centimeters).

Turbulence tends to be isotropic at the small scales, and much of the developed theory is based on isotropic, stationary, homogeneous turbulence. There are a number of situations in which turbulence is anisotropic even at small scales, however; for example, close to boundaries or in situations of strong stratification (Yamazaki 1990). The investigation of the influence of anisotropic turbulence on planktonic organisms has not yet been undertaken. As a first approximation, the experimental study of effects of small-scale turbulence on plankton has been based on the assumption of isotropic conditions even if deviations from isotropy can also be found in containers, especially close to boundaries (having there a preferred direction because the component normal to the border becomes restricted), with the size of the affected eddies decreasing toward the walls. Such situations are not considered in this article.

As a consequence of this large set of requirements, the devices used to generate turbulence in enclosed systems are diverse, depending on the organisms or processes studied, technological and logistical limitations, and choice of the researchers. Some of these systems include Couette cylinders, shaker tables, oscillating grids, and paddles (Peters and Redondo 1997, Sanford 1997)—and this list is continually increasing (e.g., Hwang and Eaton 2004, Webster et al. 2004, Warnaars et al. 2006). Most of these devices have been used for decades in other research fields before they were adopted for studies on effects of turbulence on plankton. For example, shaker tables have traditionally been used as bioreactors, to maximize the growth of cell cultures or other biological processes (e.g., Büchs 2001 and references therein), but they are also routinely used in fields not directly related to biology, such as dispersion of oil contaminants (NRC 2005). Couette cylinders are used as viscosimeters and for the study of particle aggregation under shear flow (e.g., Serra et al. 1997). Oscillating grids, a favorite of fluid dynamics experiments, have been extensively used in the study of sediment dynamics and mixing in stratified fluids (e.g., Rouse and Dodu 1955, Thompson and Turner 1975, Hopfinger and Toly 1976). To try to meet ecologically realistic conditions, these devices are often used in biological experiments using settings outside the ranges defined in their original application without a previous examination of hydrodynamics. A quantitative estimate of turbulence is not always given, and when it is, it is often based on theoretical estimations of the energy input, an approach that should be calibrated for each particular system with real measurements. Although most recent experimental studies do provide adequate quantification of turbulence levels, there are still many studies in which turbulence measurements are not conducted, particularly in the case of orbital shakers. This may interfere with the reproducibility of experiments. In addition, the technology and expertise necessary to perform such measurements are not universally available. It is therefore necessary to develop tools allowing the determination of turbulence without direct measurements, at least for the containers and systems most used in experiments with plankton.

Turbulent kinetic energy dissipation rate (ε) is the parameter most widely used to characterize turbulence in biological experiments. It is defined as the rate at which the turbulent energy is dissipated to heat due to the molecular viscosity of the fluid. According to the Kolmogorov theory of isotropic homogeneous turbulence (Kolmogorov 1941), turbulence intensity is uniquely determined by the energy dissipation rate in the inertial subrange, that is, in the range of scales between the input of turbulent mechanical energy and its dissipation as heat, in which energy is transferred from larger to smaller eddies at a constant rate. This parameter is often estimated from measurements of flow velocity fluctuations. Velocity can be measured in an Eulerian way, as for example with laser or acoustic Doppler velocimeters, or in a Lagrangian way, as in particle tracking velocimetry or particle image velocimetry.

In this article, we present turbulence measurements in two different systems commonly used in biological experiments dealing with planktonic organisms: vertically oscillating grid systems and orbital shakers. We assess turbulence in an array of different container shapes and volumes using acoustic Doppler technology for direct measurements of turbulent velocity. The aim of this study was to examine the suitability of these two types of systems to generate homogeneously distributed, stationary, and isotropic small-scale turbulence in a wide range of container volumes and measurement conditions. Additionally, we have developed statistical models to easily estimate ε within the range of conditions examined in this study, without need for direct measurements of the turbulent velocity.

Materials and procedures

Data acquisition—In all experiments, acoustic Doppler velocimeters (NDVs; Nortek A.S.) were used to measure all three Cartesian flow velocity components. NDVs use the Doppler effect for measuring velocity. A beam of 10-MHz acoustic pulses is emitted by an acoustic transducer, and the pulses scatter back from particles moving with the flow to receiving acoustic transducers. The velocity can then be derived from the measured frequency phase shift between pulses using pulse-to-pulse coherent Doppler techniques (Lhermitte and Serafin 1984). Each receiver measures the mean velocity of the particles along the direction of the axis between the transmitter and the receiver beam, i.e., along the bistatic angle. By applying a conversion matrix, it is possible

to transform the along-beam velocities into two or three orthogonal velocities. Turbulence parameters are estimated by analyzing the resulting velocity time series.

The size and shape of the sampling volume are determined by the diameter of the transducers (and therefore of the cylindrical acoustic beam) and by the length of the transmit pulse and the width of the receive window (Lohrmann et al. 1994). The size of the sampling volume may be controlled by software modifying this last parameter (McLelland and Nicholas 2000). The nominal vertical extent of the sampling volume was set at 9 mm by adjusting software configuration (Nortek 2000). The actual size and shape of the sampling volume, however, could be larger than predicted by manufacturers. For example, Finelli et al. (1999), using a Sontek acoustic Doppler velocimeter set at a sampling size of 9 mm, found the vertical sampling height to be as large as 21.5 mm. In all measurements performed within this study, the distance to the nearest boundary was always longer than 20 mm, ensuring that no boundaries are significantly affecting the results.

The frequency of acoustic pulses is between approximately 125 and 250 Hz, depending on the instrument velocity range setting (Garcia et al. 2005). The noise in a single ping is too high for practical use, and therefore a time average is output at a rate of 25 Hz. Data were acquired during at least 10 min for the oscillating grid systems and at least 5 min for the orbital shakers. There is no exact way of determining the adequate record length, as it depends on the size of the container (i.e., larger tanks need longer time series to resolve the larger eddies) and the current meter noise floor. Thus the choice of record lengths was based on previous experience (e.g., Stiansen and Sundby 2001). Two output parameters computed by the NDV were used to monitor the quality of the data: correlation and signal-to-noise ratio (SNR). The first refers to the correlation coefficient between successive velocity estimates from each receiver (Zedel et al. 1996). SNR is calculated using the signal amplitude and background noise amplitudes (McLelland and Nicholas 2000). Only time series with velocity correlations consistently >60% and with SNR consistently >20 were used (McLelland and Nicholas 2000). The resolution for each of the three velocity components from the NDV is given to be 0.1 mm s^{-1}, with a velocity bias of ±0.5% (instrument specifications).

The time lag between pulses was optimized for each measurement configuration, after visual inspection of the data, to avoid aliasing of the Doppler signal (Goring and Nikora 2002). The time lag is inversely related with maximum velocity that can be safely measured without having ambiguity errors, but also with instrument noise. Therefore, time lag was always set as high as the maximum fluid velocity in the container allowed. Time lags that could lead to pulse-to-pulse interference were avoided.

Laboratory experiments were performed with unfiltered clean tap water at approximately 20°C. To increase signal strength and reduce noise, water was seeded with hollow glass spheres with a density close to that of water and a size around 11 μm (Sphericell Hollow Glass Spheres; Potters Industries Inc.). The concentration of particles was about 50 mg L^{-1}, that is, around 7×10^4 particles mL^{-1}.

Turbulence estimation—The estimation of ε from single-point velocity time series is usually done using two different approaches. In the first approach, it is assumed that turbulence energy is mostly produced in the largest scales and transferred from large to small eddies until its dissipation occurs around the Kolmogorov microscale. It is then possible to estimate the dissipation, which mainly occurs at small scales, from the rate of input of turbulent kinetic energy (TKE) in the largest eddies (Taylor 1935):

$$\varepsilon = Au^3 l^{-1}, \tag{1}$$

where A is an universal constant assumed to be of order 1 (Tennekes and Lumley 1972), u is the root mean squared (rms) turbulent velocity, and l is the characteristic size of the largest eddies, also called integral length scale (Tennekes and Lumley 1972). The determination of l is not possible when measuring only at a single point. In oscillating grids systems, l is commonly assumed to be the mesh size (Peters and Redondo 1997), and in orbital shakers it can be assumed to be a length between the orbital diameter and the container diameter.

The second widely used approach consists in estimating ε from the energy spectrum, which is related to ε and to the wave number k in the inertial subrange

$$E(k) = \alpha\varepsilon^{2/3}k^{-5/3}, \tag{2}$$

where α is a constant of about 1.5 in the three-dimensional case and 0.5 in the one-dimensional case (Tennekes and Lumley 1972). The problem with this approach is that spatial information, needed to compute the energy spectrum, cannot be obtained from Eulerian velocity time series. When the mean flow velocity is larger than the turbulent fluctuations, however, it is possible to assume that the spatial structure of turbulence is not significantly changing as it is advected past the probe (Taylor's "frozen turbulence" hypothesis). Then, frequency can be converted from the temporal to the spatial domain in an energy spectrum. In many laboratory systems, for example in oscillating grid systems, however, net mean flows are often insignificant and therefore this assumption is broken. There are different ways to overcome this problem. For example, the probe can be moved at a large and constant velocity to have a significant relative mean flow (e.g., Thompson and Turner 1975, Hopfinger and Toly 1976).

In this study, we used the linear regression method developed by Stiansen and Sundby (2001), which is based on the inertial-advective subrange theory from Tennekes (1975). The method used the Eulerian energy spectrum by fitting a least square regression line with –5/3 slope to the inertial subrange in a log-log spectrum. Energy dissipation is then calculated by solving the equation

$$S(f) = C_f\varepsilon^{2/3}u^{2/3}f^{-5/3}, \tag{3}$$

(Tennekes 1975, modified to natural frequencies in Stiansen and Sundby 2001) where $S(f)$ is the frequency spectrum, f is the natural frequency, and C_f is a constant defined as

$$C_f = B(2\pi)^{-2/3}, \quad (4)$$

where B is a constant assumed equal to 1. Solving equation 3 gives

$$\varepsilon = 2\pi\left(\frac{10^b}{Bu^{2/3}}\right)^{3/2}, \quad (5)$$

where b is the constant of the regression line. This method allows the calculation of turbulence independently of having a net flow, and therefore can be used both in different laboratory systems and in the field. Furthermore, it filters out the instrument white noise due to the resolution of the NDV and electronic disturbances within the instrument. Dissipation was calculated for each velocity component of each whole time series. Then, the logarithmic mean of the three components was computed for an integrated estimate of ε.

In the case of oscillating grid systems, an alternative method for the estimation of ε from single-point velocity time series may be used. Dissipation may be determined as the mean rate of decay of TKE after the passage of the grid (Peters and Gross 1994). The drawback of this method is that it can be used only for oscillating grid systems and only in configurations where the grid is passing through the measurement point. An exercise of comparison between this method, the energy dissipation law method (Eq. 1), and the method from Stiansen and Sundby (2001) is presented in "Assessment and discussion."

Measurements in oscillating grid systems—In physical studies, turbulence is often generated through a grid oscillating rapidly with a small stroke. Turbulent velocities decay with the distance from the oscillating grid following a power law (Hopfinger and Toly 1976). The aim in these systems is to generate isotropic stationary turbulence at a certain distance from the grid rather than to have homogeneous conditions in the container. Similarly, in some biological experiments, stroke length is small compared to the dimensions of the tank (e.g., Estrada et al. 1987, Howarth et al. 1993, Svensen et al. 2001). This method generates spatial gradients in turbulence and is useful for looking at effects on organisms localized in layers (Utne-Palm and Stiansen 2002), to study the effect of a gradient of turbulence (Seuront et al. 2004), or to reproduce the vertical mixing in a water column (Estrada et al. 1987).

An alternative approach is to use a relatively large grid stroke, comparable to container size, and a relatively low frequency of oscillation (Peters and Gross 1994). In this case, the aim is to generate homogeneous and isotropic conditions throughout the mesocosm. We have focused our measurements on evaluating this last scenario. Three different vertically oscillating grid systems were used: one with 15-L cylindrical containers, another with 2-L cylindrical containers, and a third with 2500-L tanks (a two-gridded system). In addition, we used published data of three more systems: Peters and Gross 1994 (P&G94), Stiansen and Sundby 2001 (S&S01), and Utne-Palm and Stiansen 2002 (U&S02). Measurement conditions for all systems are listed in Table 1.

The 15-L system has been described in Peters et al. (2002). Containers were cylinders of 242 mm inner diameter and 345 mm height. Grids were made of cylindrical bars with a thickness of 3.8 mm and had a mesh size of 14 mm. Grid diameter was 216 mm, which gave a distance of 13 mm to the wall of the container. Solidity—that is, the percentage of solid surface perpendicular to the direction of the movement—was 37.8%. This system allowed changing the frequency of oscillation (between 0.034 and 0.750 Hz) and the stroke length. The lowest grid position in the experiments was always 5 mm from the bottom of the container.

The 2-L system has been described in Colomer et al. (2005). Containers were cylinders of 129 mm inner diameter and 170 mm height. Grids were as above but of 125 mm diameter. This system allowed for the use of AC gearhead motors and a variable frequency controller, which could reduce speed to 1/20th of the nominal revolutions per minute (rpm). We used two motors, of 5 and 20 nominal maximal rpm, which gave a measured frequency range between 0.065 and 0.352 Hz. Again, the lowest grid position in all experiments was 5 mm from the bottom.

In oscillating grid systems, measurement with intrusive probes is not possible unless the grid has a mesh large enough for the probe to pass through the mesh holes, which was not the case for ordinary NDVs with most of the grids used in this study. To overcome this problem in the 2- and 15-L cylinders, we used custom-made nonintrusive acoustic Doppler velocimeters designed by Nortek. The acoustic transducers were embedded into the inner wall of the containers. For each measurement point, an array of four transducers was needed to have a three-dimensional velocity series. Each array consisted of one transmitter attached to the wall and three

Table 1. Range of settings used for the measurements in the oscillating grid systems.

	15-L cylindrical container	2-L cylindrical container	2500-L tank	P&G94	S&S01	U&S02
Volume, L	7.0–15.0	2.0	2500	0.8	1600	62
Stroke radius, cm[a]	4.0–14.0	2.0–7.0	2.8–31.2	8.5	5–18.5	20
Frequency of oscillation, Hz	0.03–0.75	0.07–0.34	0.02–0.14	0.18–0.91	0.03–0.68	0.06–0.51
Measurement points, *n*	3	5	~10	5	9	26
Valid measurements, *n*	358	117	137	39	92	131

[a]The range of stroke lengths depends on the height of the water column, and therefore, on the water volume.

receivers, two of them attached to the wall at the same height than the transmitter and the third one located perpendicular to the measurement volume at the bottom of the container (Fig. 1). All receivers were equidistant to the sampling volume so that the signal would reach them at the same time. This restricted the height of the sampling measurement points, since it had to be smaller than the diameter of the container. The transducers were similar to those found in the transmitter of conventional NDVs and embedded in epoxy resin. Their acoustic frequency was 10 MHz. Containers were made of Delrin to minimize wall-reflected signals.

The grids were aligned to minimize grid bar blocking of the vertical sound beams. When the grid was at the same horizontal level as the sampling volume, however, both the transmitting signal and the two horizontal receiving signals could be partially blocked, and a drop in both velocity correlations and SNRs in the three beams could be detected. A complete blockage was not possible since the thickness of the grid (3.8 mm) was smaller than the width of the beam, which was similar to the 7-mm diameter of the transducer. The importance of this source of noise depends on the time the probe was blocked, and therefore on the frequency of oscillation and the velocity of the grid when passing through the sampling volume. This velocity depends on the position of the sampling volume, the stroke length, and the frequency of oscillation, so the relative importance of the blocking changes with the settings. The noise is more important for the smaller strokes and frequencies, that is, for the lower levels of turbulence. In general, this was a minor problem in the further analysis.

The 15-L containers had three sets of transducers (Fig. 1A), resulting in three measurement points at a height of 70, 120, and 160 mm and at a horizontal distance to the nearest wall of 70, 120, and 82 mm, respectively. The 2-L system had five sets of transducers (Fig. 1B), with measurement points at 23, 43, 64, 83, and 103 mm height and 23, 43, 64, 46, and 25 mm distance to the nearest wall, respectively.

We also evaluated a system with 2500-L cylindrical tanks (diameter 1.44 m and height 1.48 m) that was used in mesocosm experiments at the Biological Station Espegrend (University of Bergen, Norway) in 2001 and 2002. To ensure constant temperature, the tanks were further placed into larger tanks (5 m in diameter) filled with recirculating deep water from the fjord. The purpose of the mesocosm experiments was to investigate the effect of turbulence on the lower levels of the food web. Biological results are not treated in this article but can be found elsewhere (Metcalfe et al. 2004, Beauvais et al. 2006). Each system consisted of two vertically oscillating grids separated by 69 cm. The grids moved together at a given frequency powered by a pneumatic cylinder system. Changing of the stroke and the oscillation frequency controlled the generated turbulence levels. The distance from the bottom of the tank to the lowest position of the lowest grid was fixed at 25 cm in all tanks. Grid strokes ranged from 2 to 40 cm, and oscillation frequencies ranged between 0.01 and 0.07 Hz. The oscillation of the grid was not a harmonic sinusoidal motion, however. The grids took between 1 and 2 s for the up or down movement (a little bit slower upwards than downwards due to gravity) and then were at rest until the next oscillation cycle. In this case, as mesh size was large enough for a conventional acoustic Doppler sensor to pass through the holes, the measurements were conducted with a standard Nortek NDV, which was placed in different positions within the tanks.

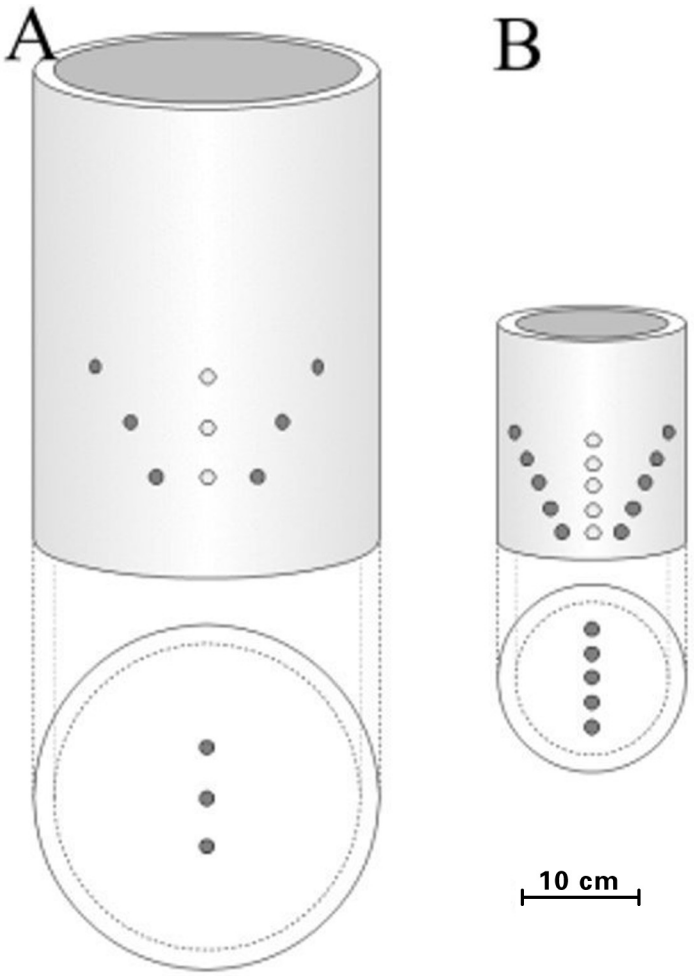

Fig. 1. Drawing of the containers used to measure oscillating grid–generated turbulence. (A) 15-L container. (B) 2-L container. Light circles are transmitter transducers and dark circles are receptors.

Measurements in orbital shaker tables—Shaker tables were some of the first devices employed in the study of turbulence effects on plankton, mainly because they are common in many marine laboratories. They have been used with planktonic organisms ranging from bacteria (Moeseneder and Herndl 1995) to copepods (e.g., Saiz and Alcaraz 1992) and have been especially important in studies with dinoflagellates (e.g., Pollingher and Zemel 1981, Berdalet 1992, Zirbel et al. 2000). They have also been used to study exopolymer particles (Stoderegger and Herndl 1999) and aggregation dynamics

(Colomer et al. 2005). In most of these studies, turbulence was not determined, or estimates were based on theoretical approaches that have not been validated with data. The determination of turbulence in these systems will allow us to place historical data into an ecological context and to evaluate the suitability of shaker tables for the study of small-scale turbulence effects on plankton.

Most measurements were done with an SBS AOS-5 orbital shaker with a range of frequencies of oscillation between 0.67 and 2.34 Hz and an orbit of 3.0 cm. Measurements were made in an array of containers commonly used in laboratories, such as glass Florence and Erlenmeyer flasks and 2.5-L polycarbonate cylindrical Nalgene bottles. Table 2 lists the different containers, water volumes, and number of measurement points. To test the effect of orbit diameter, additional measurements were done in a FinePCR SH30, with an orbital diameter of 1.4 cm, and in a Heidolph Unimax 2010, with and orbit of 2.0 cm. The measurements with these two shakers were made only in the smallest container (the 1-L Florence flask) owing to weight constraints.

Turbulence was measured with a conventional side-looking 10-MHz NDV probe. The use of nonintrusive custom-made transducer devices was disregarded because of the irregular geometry and diversity of containers. The probe was mounted on a mechanical arm attached to the shaker table, so the relative position between the sensor and the flask did not change. The number and position of measurement points were constrained by the geometry of the container, volume of water, and dimensions of the probe. Modifications were done to the mouths of the containers to allow the introduction of the probe; however, this should have no effect on the results, since this modification was well above the water level in the containers. The probe was always positioned with the axis at 90 degrees with respect to the vertical. The sampling volume of the NDV was situated 50 mm from the transmitter and was positioned toward the center of the flask to minimize vortex shedding from the instrument.

Assessment and discussion

As a comparison exercise, velocity time series from the 15-L cylindrical container in the oscillating grid system were processed using the three methods previously outlined ("Turbulence estimation"): the energy dissipation law method (Eq. 1), the linear regression method (Stiansen and Sundby 2001), and the TKE decay method (Peters and Gross 1994). For the dissipation law method, the length scale used (l in Eq. 1) was taken as the size of the mesh holes. In general, ε values obtained using linear regression method were highly correlated with those obtained with the other two methods, especially for dissipation rates higher than 10^{-4} cm^2 s^{-3} (as assessed by linear regression method, Fig. 2). The Pearson correlation coefficients between the logarithmically transformed series were in all cases >0.92 ($P < 0.001$). There were, however, significant offset differences between methods. On average, the Peters and Gross (1994) method yielded estimates 12.4 times higher than linear regression, whereas energy dissipation law estimates were 2.5 times lower.

Differences between the methods are due to misestimation of constants and appropriate length scales implied in their calculations (Stiansen and Sundby 2001). For example, the constant b in the Eulerian time spectrum (Eq. 4; Tennekes 1975), which we have set to 1 following Stiansen and Sundby (2001), may in fact be between 0.4 and 3 depending on flow conditions (Al-Homoud and Hondzo 2007). This stresses the importance of future comparison studies between different

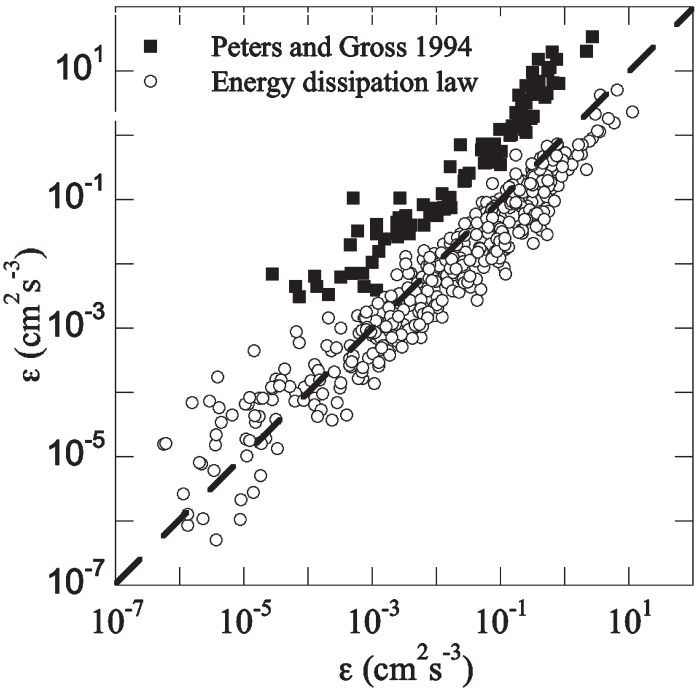

Fig. 2. Dissipation rates computed using the Peters and Gross (1994) method (left axis, solid squares) and the energy dissipation law (left axis, open circles) against dissipations computed with the linear regression method (bottom axis). Data from velocity measurements in the 15-L cylinder oscillating grid system. Plotted lines are 1:1.

Table 2. Containers used in the orbital shaker and conditions of measurement.

	4-L Florence flask	1-L Florence flask	4-L Erlenmeyer flask	2-L Nalgene bottle
Volume, L	3	0.75	3	2.6
Frequency of oscillation, Hz	1.11–2.10	0.78–2.27	0.68–2.27	0.63–2.27
Measurement points, *n*	13	2	12	4
Valid measurements, *n*	50	15	110	15

approaches and of the setting of related parameters. The estimates obtained following linear regression were considered most adequate because they gave intermediate values (among the three methods tested) and could be used for both oscillating grid systems and orbital shakers. However, observed differences imply that although the main conclusions of this study are solid given that the method is precise enough, the estimates of dissipation could be biased by as much as an order of magnitude, depending on estimation method. Turbulence levels given by different estimation methods in experimental studies of turbulence effects on plankton should therefore be interpreted within an order of magnitude.

The degree of isotropy is shown in Fig. 3, where ε measured in one horizontal component (ε_u) is plotted against ε measured

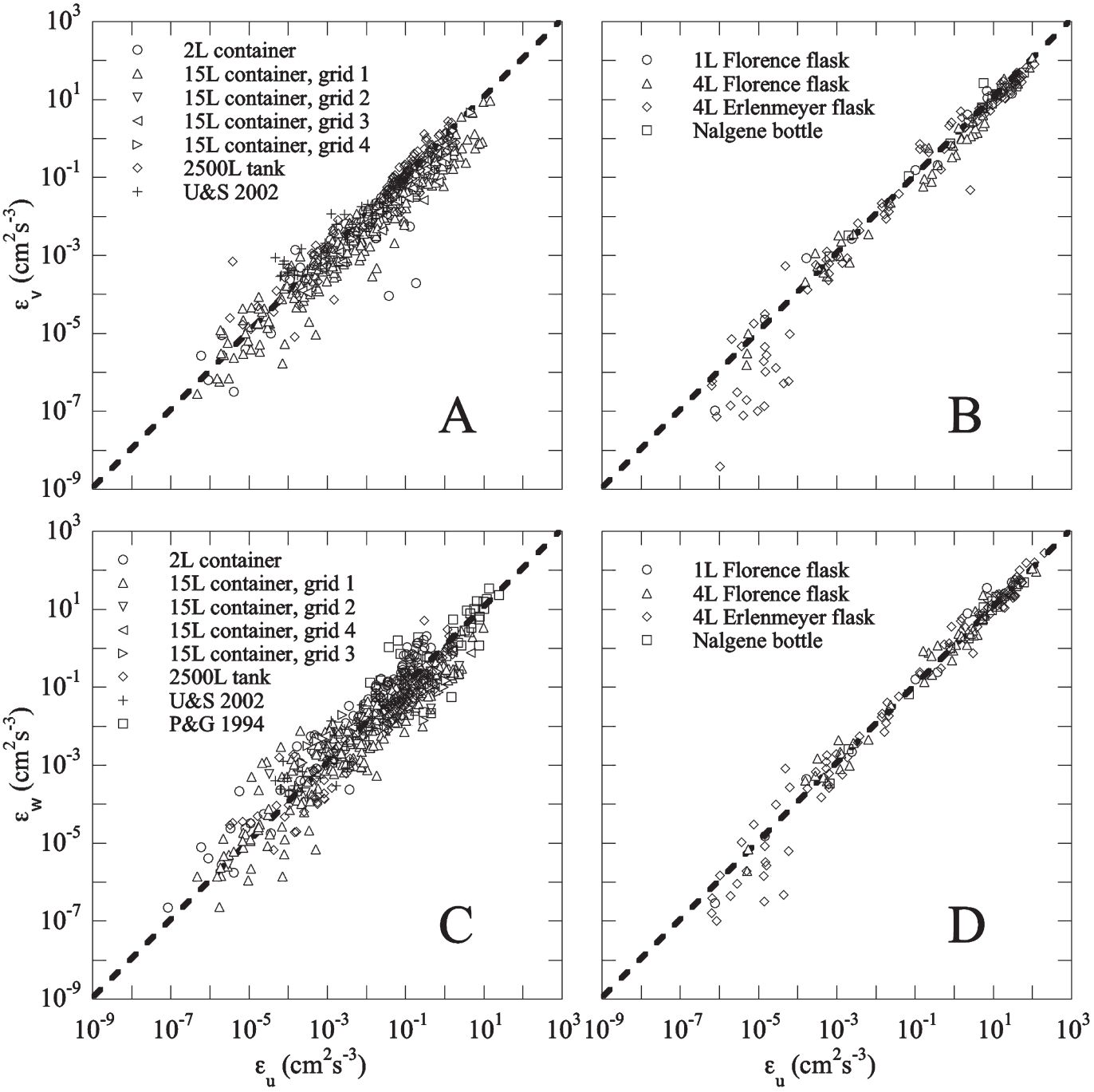

Fig. 3. Logarithmic scatterplots of ε computed from one of the horizontal velocity components and the vertical velocity component plotted against the ε computed from the other horizontal component. (A) and (C) correspond to measurements in the oscillating grid systems described in Table 1 for the different grids defined in Table 3. (B) and (D) correspond to measurements in the orbital shaker. Plotted lines are 1:1.

Table 3. Estimated drag coefficients for the grids used in this study.

Grid	Container	Mesh pattern	Mesh size, cm	Bar width, cm	Bar section	S_a cm²	Solidity %	C_d	95% CI	$A\beta C$	95% CI
1	15-L cylinder	Quadrangular	1.4	3.8	Cylindrical	139	0.38	0.084	0.005	0.020	0.006
2	15-L cylinder	Quadrangular	2.0	3.0	Cylindrical	89	0.24	0.018	0.002	0.020	0.006
3	15-L cylinder	Quadrangular	1.0	3.0	Cylindrical	150	0.41	0.020	0.003	0.020	0.006
4	15-L cylinder	Quadrangular	0.5	3.0	Rectangular	223	0.61	0.045	0.004	0.020	0.006
1	2-L cylinder	Quadrangular	1.4	3.8	Cylindrical	46	0.38	0.020	0.003	0.020	0.006
5	P&G94	Rhomboidal	0.9	1.0	Cylindrical	56	0.23	0.070	0.010	0.135	0.052
6	2500-L tank	Quadrangular	10	5	Rectangular	5474	0.40	1.521	0.360		
7	U&P02	Inner cross, with outer circle	9.4	3.0	Rectangular	337	0.52	20.240	1.430	1.191	0.299

in the other horizontal component (ε_v) and in the vertical one (ε_w) for all the available systems. Differences between components in both systems were rarely greater than an order of magnitude and fell fairly close to the 1:1 slope. To assess the effect of grid solidity on the level of isotropy reached, we performed a series of additional measurements in the 15-L grid system with three new grids (described in Table 3). Remarkably, the different oscillating grid systems generated isotropic turbulence regardless of diverse running settings, grid solidities, or geometries. In the orbital shaker system, despite the fact that a mean circular horizontal flow is established within the container, turbulence was isotropic at least for the most energetic situations (Fig. 3B and D). This isotropy is lost for $\varepsilon < 10^{-4}$ cm^2 s^{-3} in our data. Below this value the inertial subrange was difficult to identify. This is due to lower SNRs and also to the motion possibly being in the transition zone to laminar flow. Deviations within an order of magnitude for the single components of ε can usually be neglected in practical biological applications and estimations. These deviations are due to a combination of measurements and analysis uncertainty, and also intermittency and unpredictability of turbulent motion. Therefore, the components should be averaged to reduce the deviation before being used in a biological context.

The w_{rms}/u_{rms} ratios confirm the existence of nearly isotropic conditions for all the containers and both systems. In the grid systems, the ratio is between 0.44 and 2.94, with mean 1.03 and median 1.1. According to De Silva and Fernando (1994), an oscillating grid produces an isotropy ratio of 1.1–1.2. Al-Homoud and Hondzo (2007) give a range of spatially averaged isotropy ratios for an oscillating grid system between 0.92 and 0.98 (for laser Doppler velocimetry [LDV] measurements) and between 0.92 and 1.02 (for particle image velocimetry [PIV] measurements). Note that these values are for the classic case of measurements outside the oscillation volume. Our values, although they include measurements within the path of the oscillating grid, do not depart consistently from isotropy. In the orbital shaker, the rate is between 0.56 and 3.13, with mean 1.25 and median 1.3.

Time and space averaging performed by the acoustic velocimeter is a necessary step because of the Doppler noise. The smaller the sampling volume (that is, the shorter the pulse length) and the faster the sampling frequency, the lower the signal strength, and consequently, the more important the Doppler noise becomes (Lohrmann et al. 1994). Thus, although it was technically possible to set the nominal sampling volume at lower values (about 3.6 mm), this was disregarded because of the increase in Doppler noise. However, the time and space averaging of the real flow that the instrument performs limits the range of frequencies that may be resolved (Garcia et al. 2005). Only frequencies below the Nyquist frequency, defined as one-half of the sampling frequency, will be resolved in the velocity density spectrum. The velocity fluctuations with frequency higher than the sampling frequency are simply filtered out. Thus, in many cases the inertial subrange in the density spectrum is either incompletely resolved or in part below the white noise level. The linear regression model used in this study extrapolates the highest frequencies, hidden by noise and lack of resolution, from the energy in the larger vortices (Stiansen and Sundby 2001). Thus, it is possible to have an estimate of dissipation rates in conditions in which part of the inertial subrange in the spectrum is below the white noise level. In Appendix 1, two examples of temporal series, including water velocities time series and histograms, and the power spectra are presented, corresponding to the 2-L grid system (Appendix 1; Fig. 1) and the orbital shaker with a 4-L Florence flask (Appendix 1; Fig. 2).

The range of turbulence levels that could be measured by linear regression spanned more than eight orders of magnitude (from $\varepsilon < 10^{-6}$ to $> 10^{1}$ cm^2 s^{-3} with oscillating grids and from about 10^{-7} to about 10^{2} cm^2 s^{-3} with the shaker table). These ranges fit those previously measured using this method (Stiansen and Sundby 2001). The linear adjustment was done only in those cases in which an inertial subrange with a –5/3 slope was clearly identifiable in the velocity spectra. Thus, in the less energetic situations (i.e., at lowest oscillation frequencies and, in the case of grids, also at the shortest stroke lengths), in which laminar flow was more likely to be dominant, an inertial subrange

was not identified, and therefore dissipation rates could not be estimated. Sometimes in low energy conditions, the inertial subrange was clearly detected, but the number of data points valid to perform the linear regression was low, and the determination of the noise floor, dubious. As a consequence, the uncertainty of the estimates increases at the lowest values, and these must be treated with caution. Yamazaki and Osborn (1988) gave the interval 10^{-6}–10^{2} cm^2 s^{-3} for the possible energy dissipation rates in the ocean, with 10^{-4}–10^{-2} cm^2 s^{-3} as typical values for the upper mixed layer (Veth 1983, Guadayol and Peters 2006). The range of ε obtained in this assessment therefore spans the majority of turbulent situations encountered in nature.

The levels of turbulence achieved in both systems were strongly determined by the frequency of oscillation. Variability in turbulence levels was also influenced by differences in stroke length and grid geometry (for the oscillating grid systems), container volume and geometry, and position of sampling measurement points relative to the walls and bottom of the containers. Next, we present the results and discussion for each of the two systems analyzed in this study, the oscillating grid devices and the orbital shaker tables.

Oscillating grid systems

Theoretical considerations: If the turbulent flow is steady and homogeneous, the production of turbulent kinetic energy (P) must equal its dissipation (ε) (Tennekes and Lumley 1972). Following Peters and Gross (1994), in an oscillating grid system the energy input comes from the drag force D exerted by the grid in its movement:

$$D(t) = \frac{1}{2} C_d(t) \rho_w S_A v^2, \tag{6}$$

where C_d is the drag coefficient, ρ_w is the density of water, S_A is the solid area of the grid, and v is the velocity of the grid. If the grid follows a sinusoidal oscillation, velocity can be described as

$$v(t) = s\pi f \sin(2\pi f t), \tag{7}$$

where f is the frequency of oscillation and s is the stroke length, taken as the full amplitude of grid movement following Hopfinger and Toly (1976). The kinetic energy input in one oscillation is

$$E = 2 \int_0^{T/2} D(t) v(t) dt, \tag{8}$$

where T is the period of oscillation. We can easily integrate this function to obtain the total energy input during one oscillation if we assume that C_d is nearly constant with time (Higginson et al. 2003). Substituting Eqs. 6 and 7 into the equation resulting after integration of Eq. 8, we obtain

$$E = \frac{2}{3} C_d \rho_w S_A \pi^2 f^2 s^3. \tag{9}$$

The rate of production of kinetic energy per unit volume is

$$P = E T^{-1} V^{-1} \rho_w^{-1}, \tag{10}$$

where V is the volume of the container. Introducing Eq. 9 into Eq. 10, we obtain

$$P = \frac{2}{3} C_d S_A \pi^2 f^3 s^3 V^{-1}. \tag{11}$$

This equation describes the theoretical production of turbulent kinetic energy into the system assuming a harmonic sinusoidal oscillation of the grid, and therefore should be applicable to most oscillating grid systems including the 2- and 15-L systems.

In the 2500-L experimental system, which did not have a sinusoidal motion pattern, the grids moved up and down with a resting period between each half oscillation cycle. The velocity while the grid was moving can be considered constant:

$$v = s/t, \tag{12}$$

where t is the time the grid takes in each displacement (t_1 = 1.7 s upwards and t_2 = 1.0 s downwards). Therefore, the energy introduced during the oscillation is

$$E = \frac{1}{2} C_d \rho_w S_A \left(\frac{s}{t_1}\right)^3 t_1 + \frac{1}{2} C_d \rho_w S_A \left(\frac{s}{t_2}\right)^3 t_2. \tag{13}$$

Substituting Eq. 13 into Eq. 10, we obtain an estimation of P:

$$P = \frac{1}{2} C_d S_A s^3 V^{-1} f \left(t_1^{-2} + t_2^{-2}\right), \tag{14}$$

where f refers to the frequency of the complete cycle.

Distribution of ε within the experimental containers: For each oscillating grid system, all measurements of dissipation within the stroke of the grid are linearly related to the theoretical rate of energy production (Fig. 4, solid symbols). This is evidence of the homogeneity of ε within the volume of water delimited by the movement of the grid.

On the other hand, measurements done outside the movement are more variable. According to Hopfinger and Toly (1976), the root mean square turbulent velocity (u) decreases with increasing distance from the grid following this equation:

$$u = C s^{3/2} M^{1/2} z_0^{-1} f, \tag{15}$$

where C is a constant that depends on grid geometry, M is the mesh size, and z_0 is the vertical distance to the virtual origin, the point at which the longitudinal integral length scale (l in Eq. 1) becomes 0. The virtual origin can in practice be taken as the mean vertical position of the oscillating grid (Dohan and Sutherland 2002).

Taking Eq. 1, and assuming that l increases linearly with z (Thompson and Turner 1975), then

$$\varepsilon = A \beta C s^{9/2} M^{3/2} z^{-4} f^3, \tag{16}$$

where β is the constant of proportionality between l and z.

According to this, dissipation should decay as z^4 (Brumley and Jirka 1987, Bache and Rasool 1996, Al-Homoud and Hondzo 2007). Figure 5 shows the measured dissipation rates

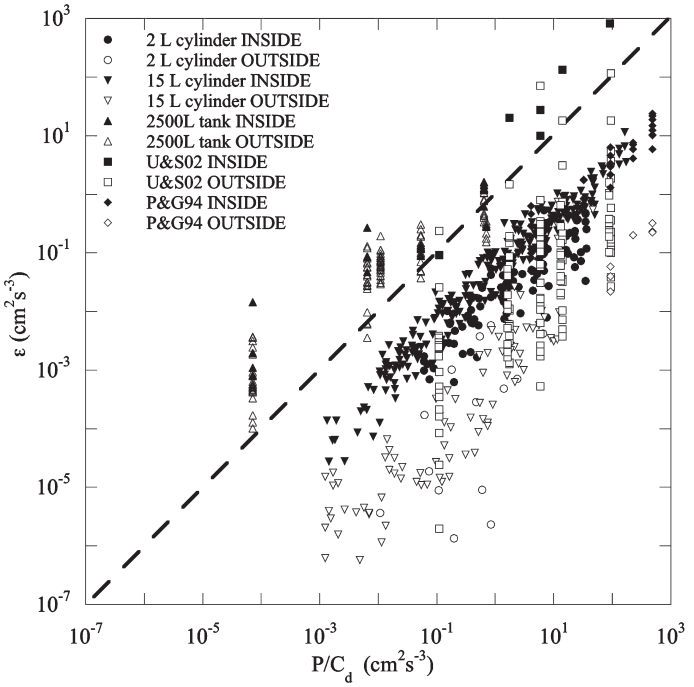

Fig. 4. Turbulent kinetic energy dissipation rate (ε) plotted against P/C_d for the oscillating grid systems, where P is the theoretical rate of kinetic energy production and C_d is the drag coefficient. Full points are measurements taken within the grid track, whereas empty points are measurements taken outside. The plotted line is $\varepsilon = P/C_d$.

against $s^{9/2}M^{3/2}z^{-4}f^3$ for those points away from the actual path of the grid. Although variability is relatively high, and even if the range of oscillating frequencies in our measurements is well below those commonly used in this kind of experiments (e.g., Thompson and Turner 1975, Hopfinger and Toly 1976, Brumley and Jirka 1987), our data are in agreement with Eq. 16 except for the 2500-L double-gridded system (Fig. 5). On the other hand, the measurements inside the track of the grid did not follow Eq. 16 in any of the systems. An estimation of $A\beta C$ for each grid was obtained by adjusting Eq. 16 (Table 3) by nonlinear least square fit.

In the double-gridded device, dissipation rates decreased with distance more slowly than predicted by Hopfinger and Toly (1976). The reason is that dissipation rates in a given point are the result of the joined effect of the two grids, which individually are likely to follow Hopfinger and Toly's model. Because decrease of ε with distance is smoother in the double-gridded system than in the single-gridded one, all other settings being equal, turbulence was more homogeneously distributed. Thus, the differences between measurements inside and outside the track of the grids were lower (Fig. 4). The difference between the highest and lowest dissipation rates within the tank in the double-gridded tank were in the order of one magnitude even when the joint stroke of the two grids was not covering the whole container.

The average values of ε in these systems are stationary if we consider time intervals larger than the oscillation period.

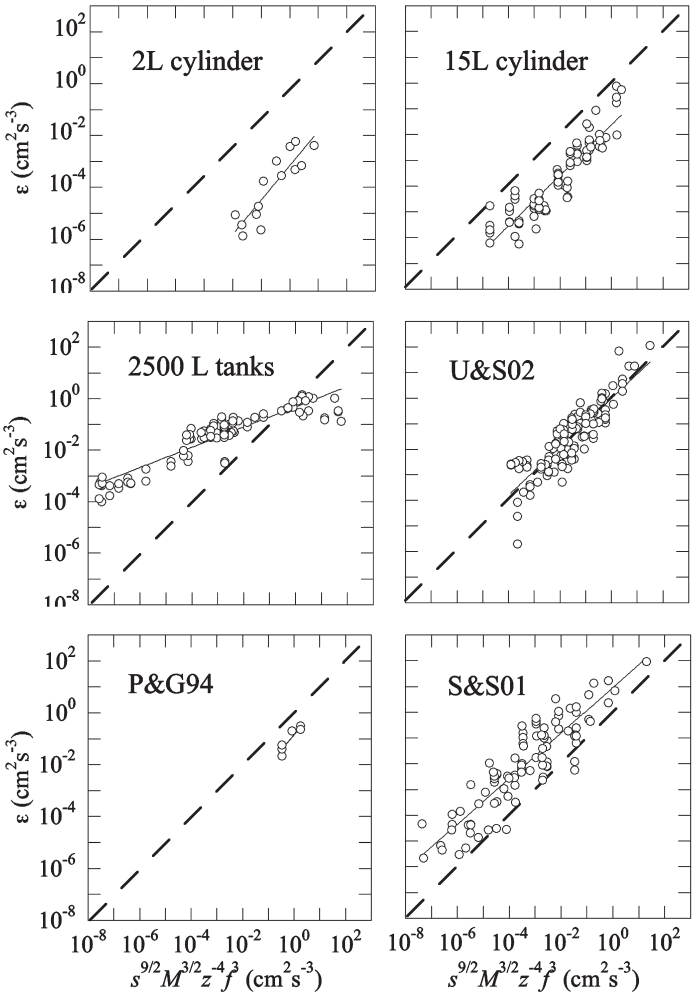

Fig. 5. Dissipation rates plotted against $s^{9/2}M^{3/2}z^{-4}f^3$ for the different oscillating grid systems examined in this study: 2-L cylinder, 15-L cylinder, 2500-L tank, U&S02, P&G94, and S&S01. Plotted discontinuous lines are 1:1. Continuous lines are the linear best fit model.

Within each oscillation period, however, there is a sinusoidal variation in the TKE. When the grid passes through the measurement point, ε is maximum, and then it decreases following a power law (Peters and Gross 1994). The estimations given are the average values that an organism will experience over time in these systems, but there is a range in turbulence intensities within each stroke, which is expected to be wider as we increase the stroke and decrease the frequency, and which will change with the position inside the container, since the velocity of the grid varies with the distance from the centre of oscillation. This sinusoidal oscillation, generally of a period of several seconds, could potentially have a significant influence on some processes with short time scales, particularly nutrient uptake processes and especially for small organisms (Peters and Marrasé 2000).

With our approximation, it is not possible to resolve fluid dynamics very close to the walls in the oscillating grid systems,

but we have shown that in most of the containers, small-scale, time-integrated turbulence is homogeneous throughout the volume covered by the grid movement. Outside this volume, it decays with distance from the virtual origin following a well-known power law (Hopfinger and Toly 1976). A smaller-scale inhomogeneity associated with the geometry of the grid cannot be dismissed.

Assessment of drag coefficient C_d: As shown, empirical data from different oscillating grid systems conforms to Eqs. 11 and 14, derived from theoretical considerations about the energy input in the system. The most relevant parameter in these equations is the drag coefficient (C_d), because it is the most difficult to assess. The drag coefficient is a function of the Reynolds number (Re). For example, the C_d of a simple cylinder is maximum at very low Re and decreases logarithmically until it reaches a plateau at Re ~1000 (Vogel 1994). Therefore, the C_d changes with the velocity of the grid and its solid area. It also depends on the geometry of the grid (e.g., the pattern of the mesh or the section of the bars) and on its surface roughness. To have precise estimates of dissipation rates using a particular grid, this should be calibrated experimentally for the range of Re implied in the system to find its particular $C_d(t)$.

However, the fact that empirical dissipation rates collapse into a line when plotted against P/C_d (Fig. 4) implies that, at least practically, the assumption of constant C_d is adequate for time-integrated estimates of dissipation rates and for the range of relatively low-frequency oscillations explored in this study. Higginson et al. (2003) found that C_d was constant for a large range of Reynolds numbers (1000–3000). According to these authors, this is an expectable result for objects of sharp edges moving in a fluid. They explained this as a consequence of boundary layer separation occurring at the edges for Reynolds numbers >100.

The empirical determination of C_d is difficult. Drag coefficient depends on several factors, such as solidity, shape of the bars forming the grid, and rugosity of the material. To calculate the C_d of a given grid, one must measure the drag force necessary to maintain the grid moving at a range of constant velocities. Alternatively, a bulk estimate of C_d for each system can be obtained from the slopes in Fig. 4. In Table 3, the drag coefficients obtained in this way for the different grids assayed in this study are listed. We include in this list several grids, similar in their mesh pattern and in the section of their bars but different in their solidities, used in the 15-L containers to evaluate the effect of grid solidity on isotropy.

Orbital shaker

Theoretical considerations: Turbulence within containers in orbital shakers is much less studied than in oscillating grids systems. Very few direct measurements have been published (Zirbel et al. 2000, Kaku et al. 2006), and no theoretical background has yet been developed. There are several possible sources for turbulence within a flask in an orbital shaker. The main is friction of water with the wall (e.g., Peters and Redondo 1997, Büchs et al. 2000) that produces instabilities of the Tollmien-Schlichting type (Peters and Redondo 1997). Therefore the angular velocity of the walls, which is a function of the frequency of oscillation and the orbit diameter, will determine the level of turbulence achieved. Our results indeed show that ε was strongly linked to the frequency of oscillation (Fig. 6), although there was a considerable scattering in the data not explained by frequency. Also, turbulence should be somewhat higher close to the walls, where the velocity shear is stronger.

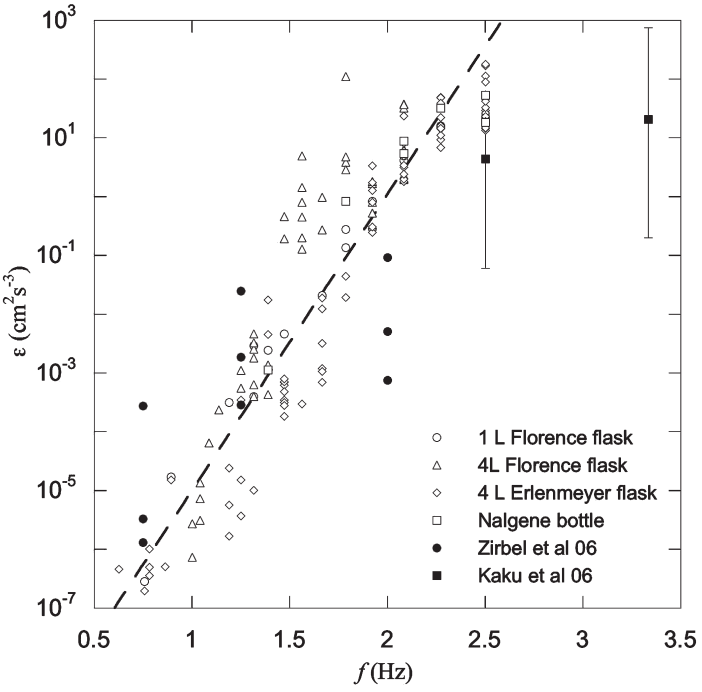

Fig. 6. Estimations of ε plotted against frequency of rotation in the orbital shaker systems. Empty points are measurements from this study; filled points are data from Zirbel et al. (2000) and Kaku et al. (2006). Plotted line is Eq. (19) fitted with the maximum likelihood method using measurements in a SBS AOS-5 orbital shaker only. Error bars indicate minimum and maximum ε values.

From our qualitative observations, water motion within the container can be divided into two general horizontal motions: (*a*) eddies of the same diameter and frequency as the orbital oscillation of the shaker and (*b*) a lower-frequency motion that follows the curvature of the container. There is also a wave of vertical displacement at the frequency of the shaker.

Empirical model: To explain the variation of ε, we fitted a general regression model (GRM; Statistica 6 software package) to the orbital shakers dataset. GRM is a statistical tool that allows the inclusion of both categorical predictor variables (e.g., type of container) and continuous predictor variables (e.g., frequency of oscillation) simultaneously within the same model. Categorical predictors are introduced into the model in the following way. A variable is created for each of the levels of a given categorical predictor except for one, which is the level against which the variables are constructed. In any of

Table 4. Summary of forward stepwise analysis for predicting $\log_{10}(\varepsilon)$ using data of orbital shaker system.

Parameter	Step	Level of effect	*B*	95% CI	SE	*P*
Intercept	0	—	–8.841	± 0.602	0.305	<0.001
F	1	—	5.051	± 0.235	0.119	<0.001
	2	4-L Florence flask	1.132	± 0.280	0.142	<0.001
	2	1-L Florence flask	–0.494	± 0.365	0.185	0.008
	2	4-L Erlenmeyer flask	–0.707	± 0.227	0.115	<0.001
D	3	—	–0.125	± 0.057	0.029	< 0.001
S	4	—	–0.095	± 0.062	0.031	0.003

$n = 183$; adjusted $R^2 = 0.91$; $F_{6,177} = 310.65$; $P < 0.0001$. The variables entered into the model were *F* (frequency of oscillation), *T* (type of container), *D* (horizontal distance to wall), and *S* (vertical distance to surface). The levels of categorical variable *C* were designed versus the treatment "2-L Nalgene bottle." *B* are the coefficients for each variable, and SE refers to these coefficients.

these numerical variables, data may take three values: 1 for the level of the variable, –1 for the level of construction, and 0 for the rest of levels. In this way, the variables are sigma-restricted (StatSoft Inc. 2006); that is, the different levels in each variable sum to zero.

We accepted the model that explained more variance with a minimum number of predictors. Forward stepwise regressions were performed with *P* values of 0.01 to enter/remove a given variable. Both backward and forward models yielded the same results. Continuous predictor variables considered for inclusion into the GRM were frequency of oscillation (*F*), horizontal distance to the wall from the measuring point (*D*), vertical distance height from the bottom to the measurement point (*H*), and vertical distance to the surface from the measurement point (*S*). The type of container (*C*) was introduced as the sigma-restricted categorical factor, and variables were constructed against the level "2.5 Nalgene bottle." Continuous predictors were tested with and without logarithmic linearization and in different combinations to find the best fit model. The dependent variable, ε, was also linearized. The final model (Table 4), with $N = 183$ valid measurements, gave an adjusted $R^2 = 0.91$.

Predictors introduced into the final model were *F*, *D*, *S*, and *C*. Frequency was found to explain more than 88% of the variance in $\log_{10}(\varepsilon)$, whereas the other predictors, even when statistically significant, explained <5% of the remaining variation. As expected (Peters and Redondo 1997), ε increased with decreasing distances to the wall, at least until D~1.5 cm, which is the minimum distance sampled in this study. Also, turbulence levels increased with decreasing *S*. The final empirical model was

$$\log_{10}(\varepsilon) = -8.84 + 5.05F - 0.13D - 0.10S + B \qquad (17)$$

where *B* is a parameter related to the type of container (Table 4). To obtain estimates of the average dissipation rates within a given container, one can numerically integrate Eq. 17 for the volume of the container. We have done so for the range of *S* and *D* covered by the measurements. The resulting equation simplifies the GRM to the following expression:

$$\log_{10}(\varepsilon) = -a + 5.05F \qquad (18)$$

Table 5. Estimations of the intercept (a) in Eq. 18 ($\log_{10}(\varepsilon) = -a + 5.05F$), for each kind of container after numerically integrating the general regression model obtained with data from orbital shaker.

Type of container	*a*
1-L Florence flask	9.9
4-L Florence flask	8.7
4-L Erlenmeyer flask	10.4
2-L Nalgene bottle	10.8
All containers	9.6

where a is a parameter different for each container. Values of a are given in Table 5. The differences between containers are remarkably low. An average fitted parameter for all the data from all the containers gives $a = 9.6 \pm 0.1$ (± 95% confidence level).

To test the effect of orbit diameter, we performed additional measurements in the 1-L Florence flask with two additional orbital shakers with orbits of 2.0 and 1.4 cm. Dissipation rates measured in the three shakers are plotted against frequency of oscillation in Fig. 7A. As expected, shakers with lower orbital diameters generated lower turbulence dissipation rates. Both parameters in Eq. 18 relate linearly with the orbital diameter. From the linear regressions between orbital diameter and parameters of Eq. 18 (Fig. 7B), it is possible to derive a general expression of $\log_{10}(\varepsilon)$ as a function of both the frequency of oscillation and the orbital diameter:

$$\log_{10}(\varepsilon) = -5.03 - 1.56\phi + (1.71 + 1.08\phi)F \qquad (19)$$

where ϕ is the orbital diameter in cm. Since we could not use the whole set of containers in the three different shaker tables, this expression does not account for the variability due to type of containers and distance from the wall.

Discussion on orbital shaker results: The orbital shaker study was designed to look at differences between the containers; however, it was possible to detect a significant influence of wall proximity. Other variables, such as the type of motion (e.g., orbital vs. reciprocal) or the fluid volume within a given container should be the subject of future studies. Moreover, all containers had a circular base. Results will be

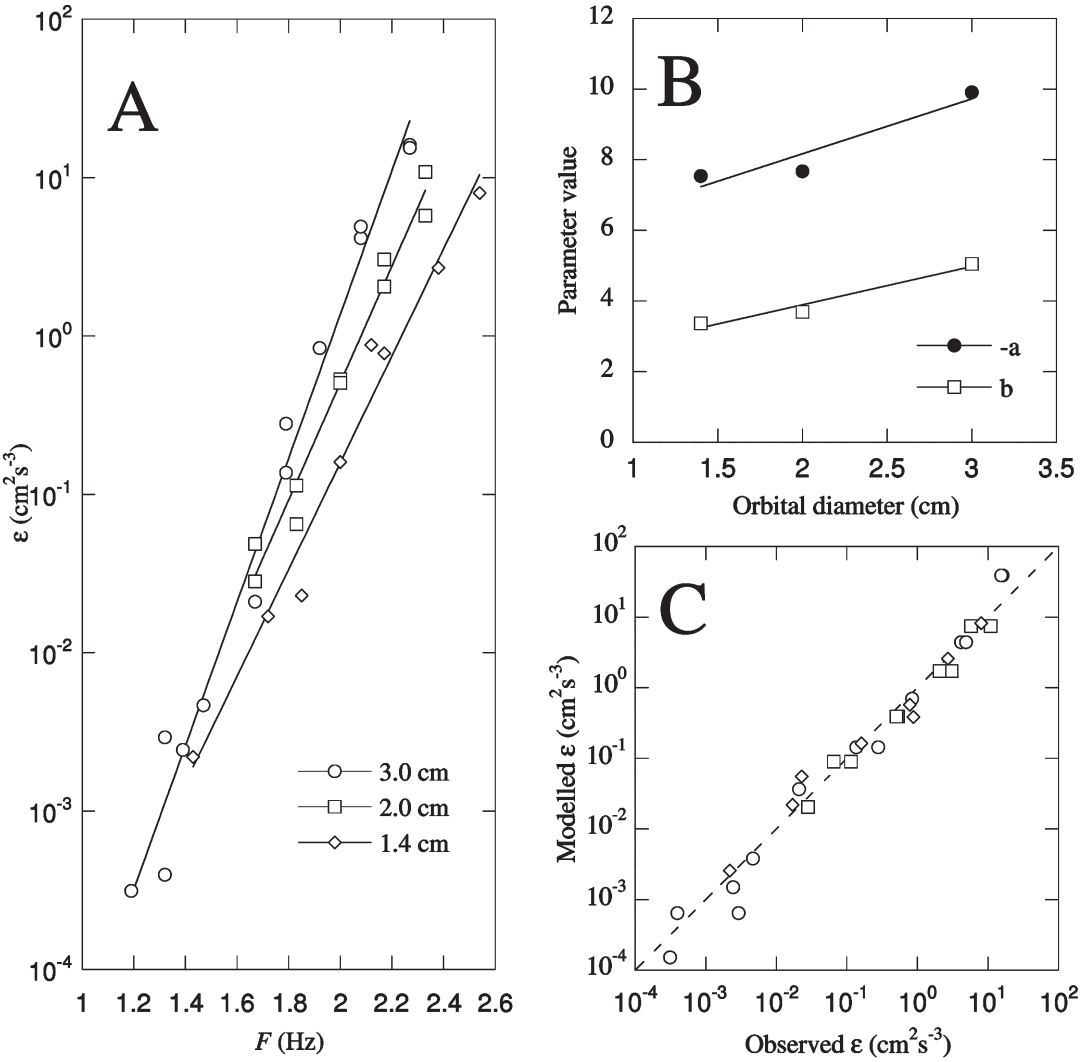

Fig. 7. Study of the effect of orbital diameter in a 1-L Florence flask. (A) Measured dissipation rates against frequency of oscillation. Plotted lines are best fit regression lines ($\log_{10}(\varepsilon) = a + bf$) for each orbital diameter tested (1.4, 2.0, and 3.0 cm). (B) Parameters a and b from the regression models plotted in (A), against orbital diameter. Lines are best fitted linear regressions. (C) Measured against modeled ε using Eq. 19.

different in containers with corners or irregular shapes at the base (Kaku et al. 2006).

The frequency of oscillation was the best predictor for dissipation rates when orbit diameter was held constant. This is consistent with friction of water with the wall being the main source of turbulence in the container. In a minor degree, geometrical parameters such as the height of the container or its horizontal shape are also affecting the turbulence levels.

Equation 18 gives an average value of dissipation within the tanks, i.e., the mean turbulence level an organism subjected to a given experimental condition is likely to experience. But turbulence is not completely homogeneous, since it depends on the distance to the side and bottom walls. When integrating the dissipation rates for the full container, this dependence on the distance to the wall may be critical, because the volume increases with the radius. This means that for the same orbital diameter and frequency of oscillations, average ε will increase nonlinearly with the container diameter. It means also that the larger this diameter, the wider the range of ε reached within the container. From the empirical model (Table 4), it is possible to infer a 10-fold difference in dissipation between points separated 10 cm.

Measurements of fluid motion in tanks on orbital shaker tables are very scarce. In Fig. 6 we have plotted the available datasets (Zirbel et al. 2000, Kaku et al. 2006), together with our measurements. Zirbel et al. (2000) measured shear stress in 125-mL flasks with 60 mL water for a shaker table with an orbit of 2.54 cm. The horizontal velocity field was measured with a two-component DPIV (digital particle image velocimetry) system. They measured the velocity field at three different rotation frequencies (0.75, 1.25, and 2 Hz). Their results also show a decrease in turbulence with increasing distance to the

wall and a strong dependence with the frequency of rotation. However, their measurements depart from the empirical relationship found in this study, at least at the highest frequency. Measurement conditions were quite different from ours, since they used a much smaller container and fluid volume than ours. According to Zirbel et al. (2000), there were some limitations associated with the fact that the measurement plane is horizontal and with interactions between the illumination and the glass of the flask. Differences from Zirbel et al. (2000) measurements can also come from a hypothetical bias in our data due to vortex shedding from the intrusive probe. This was tested by placing the 15-L cylindrical container with the wall-mounted velocity sensors used for the oscillating grid system on the orbital shaker. No change was detectable in measured ε from the wall-mounted sensors when the side-looking NDV probe was introduced in the tank. This test is not entirely conclusive, however, since effect of the intrusive probe could be very different in containers of different shapes and sizes. Another factor that could explain the difference is the orbit, which was 5 mm larger in our case.

Kaku et al. (2006) measured turbulence in a 150-mL Erlenmeyer flask with 120 mL water in a shaker with an orbital diameter of 1.9 cm oscillating at 2.5 and 3.3 Hz. Measurements were conducted using a hot wire anemometer with a sampling frequency of 1000 Hz during 10 s at 2-mm intervals. Their data fall below what should be expected from extrapolation of the empirical model to higher frequencies (Fig. 5), which is reasonable since orbital diameter was lower than ours. This bias may also be related to the determination of dissipation rates, because they used the energy dissipation model, which gives lowest estimations (Fig. 2), at least in the case of grid systems.

The use of containers with different and relatively complex shapes makes it difficult to relate empirical results with theoretical estimations based on energy input in orbital shakers. Colomer et al. (2005) assumed ε to be proportional to f^3, in analogy with impeller-stirred tanks. According to Büchs et al. (2000), the power consumption of a shaking system should be scaled to $f^{2.8}$. Our measurements, however, in agreement with the other few previous direct measurements (Zirbel et al. 2000, Kaku et al. 2006), show a much steeper relationship. Thus, the 2.8 relationship, which has been empirically tested (Büchs et al. 2000, Peter et al. 2006), seems to hold only for the range of conditions usual in shaking bioreactors, in which the volume of fluid is <20% of the nominal flask volume (e.g., Büchs et al. 2000), and the frequency of oscillation is usually much higher. Under these conditions, the kinetic energy production rate is very high, typically above 5×10^3 cm^2 s^{-3}, and the bottom of the flask runs dry (Büchs et al. 2000).

Following this analogy with tanks mixed by impellers, ε has been suggested to be inversely proportional to V. By contrast, we did not found a significant effect of V on turbulence generated by an orbital shaker. Note that the effect of water volume has not been systematically addressed here: it would require a set of measurements with a range of different water volumes for the same tank. This effort seems partly irrelevant, as frequency alone can explain so much variance despite the use of different types of containers, each one with different water volumes.

Other parameters, such as orbit diameters or free surface, could affect the results. Duetz and Whitholt (2001) observed large differences in fluid motion in a container subjected to two different orbit diameters (2.5 and 5 cm), but to our knowledge no one has quantitatively addressed this aspect. We have extended our set of measurements to test for the possible effect of orbital diameter. As expected, dissipation rates increase with the diameter of the orbital oscillation. Equation 19 offers a first approximation to this problem; however, this relationship must be taken with care because it is based on only three different orbital diameters and one type of container. Subsequent studies must extend the range of orbital diameters and experimental containers which this study could not cover, to confirm and develop such a relationship. In general, frequency alone remains the best predictor of dissipation rate regardless of fluid volume and container shape.

Comments and recommendations

There are some published evaluations of turbulence in agitated tanks used in experiments with planktonic organisms, but more measurements are necessary, especially in orbital shaker systems. Our results show that oscillating grid and shaker table systems attain a wide range of turbulence levels, covering well the turbulence values found in the field (Peters and Marrasé 2000). Despite that there is a dominant direction in the generation of movement in both kinds of systems, conditions are fairly isotropic in all tested container types and energy input conditions, with the exception of low energetic situations in orbital shakers where isotropy can be lost. Also, there is a fine line between laminar and turbulent conditions. Therefore, we do not recommend frequencies below about 1 Hz for studies on effects of turbulence on plankton in orbital shakers.

Oscillating grids produce more homogeneous conditions than orbital shakers, as long as the grid is moving throughout the container. When designing experiments with plankton, it is therefore especially important to use the maximum possible stroke in these systems, unless the objective is to study the effect of nonhomogeneous turbulence (i.e., gradient). One constraint lies at low oscillation frequencies, since organisms will experience intermittent pulses of turbulence followed by periods of calmer conditions. The system should tend to maximize both the stroke amplitude and the frequency of oscillation, to approximate homogeneous and stationary conditions. The upper constraint is the generation of natural levels of turbulence. In addition, organisms with enough swimming capability (e.g., fish larvae, copepods, dinoflagellates) could escape the movement of the grid. Consequently, this system should be a first choice mainly for the smallest plankton, unless the systems are large and plankton stays in a limited area of the tank.

Two main conclusions that can be derived from the grid oscillation systems analysis are that (*a*) the dissipation rate can be assessed from theoretical considerations and (*b*) C_d can be considered constant for practical biological applications. It is still not possible to predict C_d from geometric considerations, since it depends not only on solidity, but also on the size and shape of the bars that conform the grid, its geometry, and its smoothness. We have presented in Table 3 a set of different C_d values obtained from different grids as a guide for future studies. We strongly recommend using similar grids or other models previously calibrated in future studies. More effort should be put into calibrating different grids under the oscillation conditions used in biological experiments. An estimation of average dissipation rate within the volume covered by the grid movement can be obtained using Eq. 11 (or Eq. 14 for nonsinusoidal movement). The decay of turbulence away from the zone of the grid is predicted using Eq. 16 derived from Hopfinger and Toly (1976).

In orbital shakers, as turbulence depends on geometrical parameters such as the distance from the wall and the bottom, there is always a gradient of dissipation. The effect is rather small, but it can account for an order of magnitude of difference in ε between the wall and the center of the flask. Moreover, superimposed to the turbulent eddies, there is always a strong dominant flow that could affect the distribution and behavior of the organisms. Small and narrow containers should minimize these inhomogeneities. To obtain an integrated average value for a given container on an orbital shaker, the best way is to integrate numerically the empirical model presented in Table 4. If the type of container used is different from the ones of this study, one can use Eq. 18 with a = 9.6 (Table 5) to estimate a bulk value of the dissipation. For shaker tables with a different orbit, Eq. 19 gives the dissipation rates in a 1-L container depending on frequency and orbital diameter. A summary of the equations to calculate ε in oscillating grids as well as in orbital shakers, along with the ranges of conditions tested within this study, is provided in Table 6.

In summary, the range of dissipations measured in both systems is comparable to the natural ranges of turbulence. Furthermore, both systems produce fairly isotropic small-scale turbulence, regardless of a dominant direction of forcing. Conditions are more spatially homogeneous in oscillating grid systems than in orbital shakers, where a significant radial gradient exists. However, the differences may be kept within an order of magnitude by choosing proper container dimensions. Thus, with the cautions and limitations mentioned here, both systems are adequate for the study of effects of small-scale turbulence on plankton organisms and communities, and especially for organisms with relatively limited mobility and small size. Equations summarized in Table 6 can easily be used to

Table 6. Estimation of average dissipation rates in oscillating grid and orbital shaker systems: summary of the main equations and their conditions of applicability.

System	Conditions		Equation	Parameters	Tested ranges
Vertically oscillating grid	Within the grid path	Sinusoidal velocity	$P = \frac{2}{3} C_d S_A \pi^2 f^3 s^3 V^{-1}$ (Eq. 11)	C_d = drag coefficient (see Table 3) S_A = surface area (cm²) f = frequency (s⁻¹) s = stroke length (cm) V = volume (cm³) t_1 = time upwards (s) t_2 = time downwards (s) M = mesh size (cm) z = distance from the center of oscillation (cm) $A\beta C$ are constants (see Table 3)	S_A = [46–337] f = [0.03–0.91] s = [4.0–28.0] V = [7.8 × 10²–6.1 × 10⁴] M = [0.5–9.4]
		Constant velocity	$P = \frac{1}{2} C_d S_A s^3 V^{-1} f \left(t_1^{-2} + t_2^{-2}\right)$ (Eq. 14)		S_A = 5474 f = [0.02–0.14] s = [2.8-40.0] V = 2.5 × 10⁷ M = 10
	Outside the grid path		$\varepsilon = A\beta C s^{9/2} M^{3/2} z^{-4} f^3$ (Eq. 16)		S_A = [46–6476] f = [0.03–0.91] s = [2.8–40.0] V = [7.85 × 10²–1.6 × 10⁶] M = [0.9–10] z = [1–73]
Orbital shaker	General case		$\log_{10}(\varepsilon) = -5.03 - 1.56\phi + (1.71 + 1.08\phi)F$ (Eq. 19)	F = frequency (s⁻¹) D = horizontal distance to the wall (cm) S = vertical distance to the surface (cm) B is a constant specific of each container (see Table 4) ϕ = orbit diameter (cm)	F = [1.19–2.54] ϕ = [1.4–3.0] D = [2.74–2.99] S = [2.10–3.60]
	Special case (orbit 3.0 cm)		$\log_{10}(\varepsilon) = -8.84 + 5.05F - 0.13D - 0.10S + B$ (Eq. 17)		F = [0.63–2.27] ϕ = 3.0 D = [0.37–9.62] S = [2.10–17.00]

assess average dissipation rates in oscillating grid systems and orbital shakers within the ranges of conditions explored in this article.

References

Al-Homoud, A., and M. Hondzo. 2007. Energy dissipation estimates in oscillating grid setup: LDV and PIV measurements. Environ. Fluid Mech. 7:143-158.

Bache, D. H., and E. Rasool. 1996. Measurement of the rate of energy dissipation around an oscillating grid by an energy balance approach. Chem. Eng. J. 63:105-115.

Berdalet, E. 1992. Effects of turbulence on the marine dinoflagellate *Gymnodinium nelsonii*. J. Phycol. 28:267-272.

Beauvais, S., M. L. Pedrotti, J. Egge, K. Iversen, and C. Marrasé. 2006. Effects of turbulence on TEP dynamics under contrasting nutrient conditions: implications for aggregation and sedimentation processes. Mar. Ecol. Progr. Ser. 323:47-57.

Brumley, B. H., and G. H. Jirka. 1987. Near-surface turbulence in a grid-stirred tank. J. Fluid Mech. 183:235-263.

Büchs, J. 2001. Introduction to advantages and problems of shaken cultures. Biochem. Eng. J. 7:91-98.

Büchs, J., U. Maier, C. Milbradt, and Zoels, B. 2000. Power consumption in shaking flasks on rotary shaking machines: I. Power consumption measurement in unbaffled flasks at low liquid viscosity. Biotechnol. Bioeng. 68:589-593.

Colomer, J., F. Peters, and C. Marrasé. 2005. Experimental analysis of coagulation of particles under low-shear flow. Water Res. (Oxf.) 39:2994-3000.

De Silva, I. P. D., and H. J. S. Fernando. 1994. Oscillating grids as a source of nearly isotropic turbulence. Phys. Fluids 6:2455-2464.

Dohan, K., and B. R. Sutherland. 2002. Turbulence time-scales in mixing box experiments. Exp. Fluids 33:706-719.

Duetz, W. A., and B. Witholt. 2001. Effectiveness of orbital shaking for the aeration of suspended bacterial cultures in square-deepwell microtiter plates. Biochem. Eng. J. 7:113-115.

Estrada, M., M. Alcaraz, and C. Marrasé. 1987. Effects of turbulence on the composition of phytoplankton assemblages in marine microcosms. Mar. Ecol. Prog. Ser. 38:267-281.

Finelli, C.M., Hart, D.D., and D.M. Fonseca. 1999. Evaluating the spatial resolution of an acoustic Doppler velocimeter and the consequences for measuring near-bed flows. Limnol. Oceanogr. 44:1793-1801.

Garcia, C. M., M. I. Cantero, Y. Niño, and M. H. Garcia. 2005. Turbulence measurements with acoustic Doppler velocimeters. J. Hydraul. Eng. (N.Y.) 131:1062-1073.

Goring, D. G., and V. I. Nikora. 2002. Despiking acoustic Doppler velocimeter data. J. Hydraul. Eng. (N.Y.) 128:117-126.

Guadayol, Ò., and F. Peters. 2006. Analysis of wind events in a coastal area: a tool for assessing turbulence variability for studies on plankton. Sci. Mar. 70:9-20.

Higginson, R. C., S. B. Dalziel, and P. F. Linden. 2003. The drag on a vertically moving grid of bars in a linearly stratified fluid. Exp. Fluids 34:678-686.

Hopfinger, E. J., and J. A. Toly. 1976. Spatially decaying turbulence and its relation to mixing across density interfaces. J. Fluid. Mech. 78:175-188.

Howarth, R. W., T. Butler, K. Lunde, D. Swaney, and C. H. Chu. 1993. Turbulence and planktonic nitrogen fixation: a mesocosm experiment. Limnol. Oceanogr. 38:1696-1711.

Hwang, W., and J. K. Eaton. 2004. Creating homogeneous and isotropic turbulence without a mean flow. Exp. Fluids 36:444-454.

Kaku, V. J., Boufadel, M. C., and A. D. Venosa. 2006. Evaluation of mixing energy in laboratory flasks used for dispersant effectiveness testing. J. Envir. Eng. 132:93-101.

Kolmogorov, A. N. 1941. The local structure of turbulence in incompressible viscous fluid for very large Reynolds number. Dokl. Akad. Nauk SSSR 30:9-13. (Reprinted in Proc. Roy. Soc. Lond. A 434:9-13, 1991).

Lhermitte, R., and R. Serafin. 1984. Pulse-to-pulse coherent Doppler sonar signal processing techniques. J. Atmos. Ocean. Technol. 1:293-308.

Lohrman, A., Cabrera, R., and N.C. Kraus. 1994. Acoustic-Doppler velocimeter (ADV) for laboratory use. Proceedings of the Symposium on Fundamentals and Advancements in Hydraulic Measurements and Experimentation, American Society of Civil Engineers, Buffalo, NY (1994), pp 351-365.

McLelland, S. J., and A. P. Nicholas. 2000. A new method for evaluating errors in high-frequency ADV measurements. Hydrol. Process. 14:351-366.

Metcalfe, A. M., T. J. Pedley, and T. F. Thingstad. 2004. Incorporating turbulence into a planktonic foodweb model. J. Mar. Syst. 49:105-122.

Moeseneder, M. M., and G. J. Herndl. 1995. Influence of turbulence on bacterial production in the sea. Limnol. Oceanogr. 40:1466-1473.

Nortek AS. 2000. Nortek 10 Mhz velocimeter operations manual. Document N3000-100/Rev.c/01.11.2000, 28 pp.

NRC, Committee on Understanding Oil Spill Dispersants: Efficacy and Effects. 2005. Oil spill dispersants: efficacy and effects. http://www.nap.edu/catalog.php?record_id=11283#toc. (Accessed March 21, 2009.)

Peter, C. P., Y. Suzuki, and J. Büchs (2006) Hydromechanical stress in shake flasks: correlation for the maximum local energy dissipation rate. Biotechnol. Bioeng. 93:1164-1176.

Peters, F., and T. Gross. 1994. Increased grazing rates of microplankton in response to small-scale turbulence. Mar. Ecol. Prog. Ser. 115:299-307.

Peters, F., and J. M. Redondo. 1997. Turbulence generation and measurement: application to studies on plankton. In: C. Marrasé, E. Saiz, and J. M. Redondo (eds.), Lectures on plankton and turbulence. Sci. Mar. 61 (Suppl. 1):205-228.

Peters, F., and C. Marrasé. 2000. Effects of turbulence on plankton: an overview of experimental evidence and some theoretical considerations. Mar. Ecol. Prog. Ser. 205:291-306.

Peters, F., C. Marrasé, H. Havskum, F. Rassoulzadegan, J. Dolan, M. Alcaraz, and J. M. Gasol. 2002. Turbulence and the

microbial food web: effects on bacterial losses to predation and on community structure. J. Plankton Res. 24:321-331.

Pollingher, U., and E. Zemel. 1981. In situ and experimental evidence of the influence of turbulence on cell division processes of *Peridinium cinctum forma westii* (Lemm.) Lefèvre. Br. Phycol. J. 16:281-287.

Rouse, H., and J. Dodu. 1955. Diffusion turbulente á travers une discontinuité de densité. La Houille Blanche 4:522-532.

Seuront, L., H. Yamazaki, and S. Souissi. 2004. Hydrodynamic disturbance and zooplankton swimming behavior. Zool. Stud. 43:376-387.

Saiz, E., and M. Alcaraz. 1992. Enhanced excretion rates induced by small-scale turbulence in Acartia (Copepoda: Calanoida). J. Plankton Res. 14:681-689.

Sanford, L. P. 1997. Turbulent mixing in experimental ecosystem studies. Mar. Ecol. Prog. Ser. 161:265-293.

Serra, T., Colomer, J., and X. Casamitjana. 1997. Aggregation and breakup of particles in a shear flow. J. Colloid Interface Sci. 187:466-473.

StatSoft, Inc. 2006. Electronic statistics textbook. Tulsa, OK: StatSoft. http://www.statsoft.com/textbook/stathome.html. (Accessed March 21, 2009.)

Stiansen, J. E., and S. Sundby. 2001. Improved methods for generating and estimating turbulence in tanks suitable for fish larvae experiments. Sci. Mar. 65:151-167.

Stoderegger, K. E., and G. J. Herndl. 1999. Production of exopolymer particles by marine bacterioplankton under contrasting turbulence conditions. Mar. Ecol. Prog. Ser. 189:9-16.

Svensen, C., J. K. Egge, and J. E. Stiansen. 2001. Can silicate and turbulence regulate the vertical flux of biogenic matter? A mesocosm study. Mar. Ecol. Progr. Ser. 217:67-80.

Taylor, G. I. 1935. Statistical theory of turbulence. Proc. Roy. Soc. Lon. A 151:421-444.

Tennekes, H. 1975. Eulerian and lagrangian time microscales in isotropic turbulence. J. Fluid Mech. 67:561-567.

Tennekes, H., and J. L. Lumley. 1972. A first course in turbulence. Cambridge, MA: MIT Press, 300 pp.

Thompson, S. M., and J. S. Turner. 1975. Mixing across an interface due to turbulence generated by an oscillating grid. J. Fluid Mech. 67:349-368.

Utne-Palm, A. C., and J. E. Stiansen. 2002. Effect of larval ontogeny, turbulence and light on prey attack rate and swimming activity in herring larvae. J. Exp. Mar. Biol. Ecol. 268:147-170.

Veth, C. 1983. Turbulence measurements in the stratified central North Sea with laser-Doppler velocimeter system. In: J. Südermann and W. Lenz (eds.), North Sea dynamics. Berlin: Springer-Verlag, p. 412-428.

Vogel, S. 1994. Life in moving fluids: the physical biology of flow. 2nd edition. Princeton, NJ: Princeton University Press, 467 pp.

Warnaars, T. A., M. Hondzo, and M. A. Carper. 2006. A desktop apparatus for studying interactions between microorganisms and small-scale fluid motion. Hydrobiologia 563:431-443.

Webster, D. R., A. Brathwaite, and J. Yen. 2004. A novel laboratory apparatus for simulating isotropic oceanic turbulence at low Reynolds number. Limnol. Oceanogr. Methods 2:1-12.

Yamazaki, H., and T. R. Osborn. 1988. Review of oceanic turbulence: implications for biodynamics. In: B. J. Rothschild (ed.), Towards a theory on biological-physical interactions in the world ocean. Dordrecht, Germany: Kluwer Academic, p. 215-234.

Yamazaki, H. 1990. Stratified turbulence near a critical dissipation rate. J. Phys. Oceanogr. 20:1583-1598.

Zedel, L., A. E. Hay, R. Cabrera, and A. Lohrmann. 1996. Performance of a single-beam pulse-to-pulse coherent Doppler profiler. IEEE J Oceanic Eng. 21:290-297.

Zirbel, M. J., F. Veron, and M. I. Latz. 2000. The reversible effect of flow on the morphology of *Ceratocorys horrida* (Peridiniales, Dinophyta). J. Phycol. 36:46-58.

Submitted 19 November 2007
Revised 28 November 2008
Accepted 18 February 2009